STRUCTURAL BIOLOGY

Volume 78 (2022)

Supporting information for article:

Atomic resolution studies of S1 nuclease complexes reveal details of RNA interaction with the enzyme despite multiple lattice-translocation defects

Kristýna Adámková, Tomáš Kovaľ, Lars H. Østergaard, Jarmila Dušková, Martin Malý, Leona Švecová, Tereza Skálová, Petr Kolenko and Jan Dohnálek

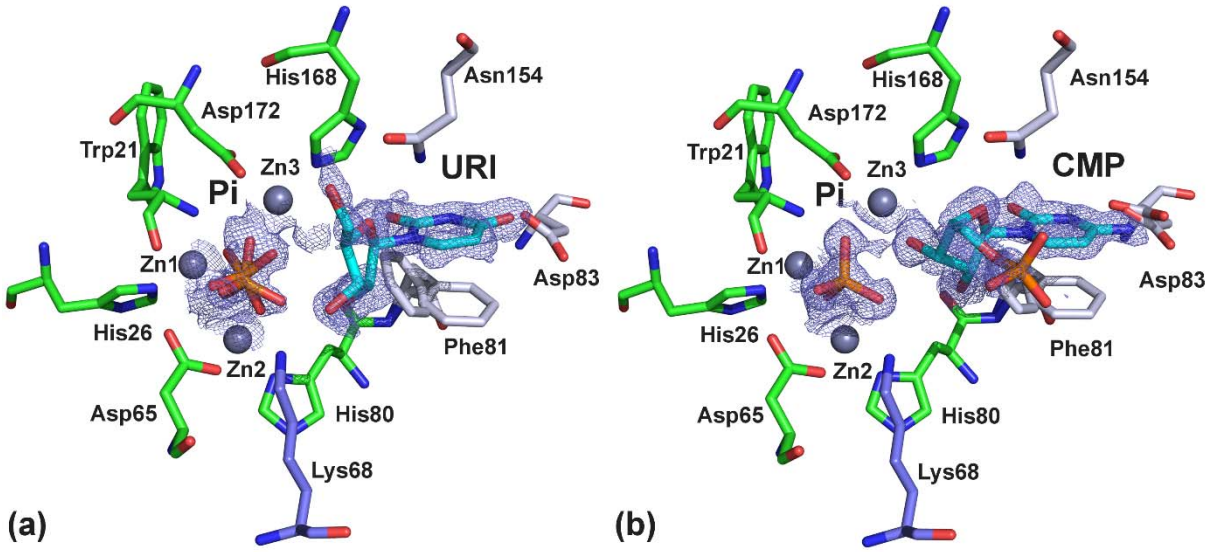

Figure S1 The ligand binding in the active site of S1-URI and S1-CMP with 2mF_o–DF_c (blue mesh) composite omit map around ligands at 1σ level. (a) The active site of the S1-URI complex with bound phosphate ion (Pi, phosphorus in orange) and uridine (URI, carbon in cyan) and (b) the active site of S1-CMP with bound phosphate ion (Pi, phosphorus in orange) and cytidine-5′-monophosphate (CMP, carbon in cyan). Active site is composed of zinc ions (grey spheres) coordinated by nine amino acids (carbon in green), NBS1 site (carbon in light blue), and one positive residue Lys68 (carbon in blue). The molecular graphics was created using *PyMOL* (Schrödinger) and the composite omit maps were generated in *Phenix* (Adams *et al.*, 2010) using the refinement option and the final corrected data.

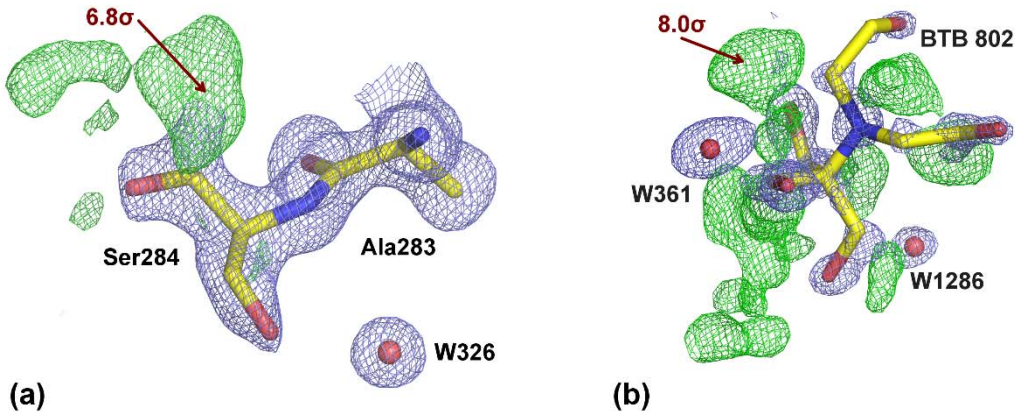

Figure S2 The highest positive residual difference density maxima of the S1-URI and S1-CMP structures. (a) The highest mF_o–DF_c peak of S1-URI structure at 6.8σ level indicating uninterpretable C-terminus of the protein chain and (b) the highest mF_o–DF_c peak of the S1-CMP structure at 8.0σ level – most likely a mixture of alternative conformations of a Bis-Tris molecule. 2mF_o–DF_c electron density (blue mesh) is contoured at 1σ level and mF_o–DF_c difference electron density (green and red mesh) is contoured at 3σ level (protein in sticks with carbon in yellow, water molecules as red spheres). The molecular graphics was created using *PyMOL* (Schrödinger).

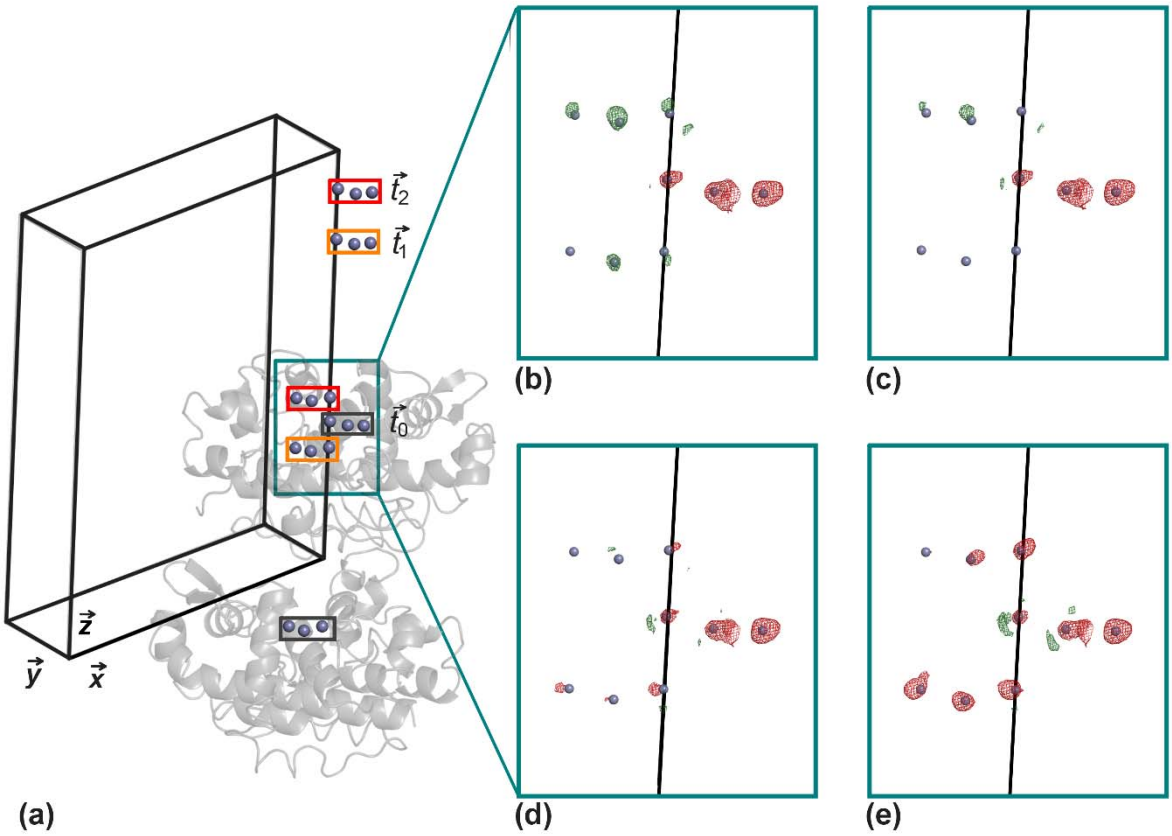

Figure S3 Two-vector correction of multiple lattice-translocation defect, which leads to insufficient LTD correction of S1-URI data. (a) Unit cell of crystal structure S1-URI with enzyme molecules (grey cartoon) and zinc ions (grey spheres, grey rectangles) in original positions ($\mathbf{t}_0$) and in the two translated positions using translation vectors $\mathbf{t}_1$ = (0, 0, 0.4380) (orange rectangles) and $\mathbf{t}_2$ = (0, 0, 0.5620) (red rectangles). (b-e) Detailed view with mF_o–DF_c difference density contoured at 3σ level around the zinc ions (red and green mesh) (b) after refinement against corrected data with k_1 = 0.04 and k_2 = 0.05, (c) after refinement against corrected data with k_1 = 0.05 and k_2 = 0.06, (d) after refinement against corrected data with k_1 = 0.06 and k_2 = 0.07, and (e) after refinement against corrected data with k_1 = 0.07 and k_2 = 0.08. The molecular graphics was created using *PyMOL* (Schrödinger).

Table S1 S1-URI data two-vector correction parameters and comparison of refinement statistics provided by *Refmac5* (Murshudov *et al.*, 2011) after data correction with only two translation vectors $\mathbf{t}_1 = (0, 0, 0.438)$ and $\mathbf{t}_2 = (0, 0, 0.562)$.

Parameters k_1 and k_2 correspond to translation vectors $\mathbf{t}_1$ and $\mathbf{t}_2$. Translation vectors are in fractional coordinates.

S1-URI		Data correction			
	uncorrected	Correction 1 (Fig. S3b)	Correction 2 (Fig. S3c)	Correction 3 (Fig. S3d)	Correction 4 (Fig. S3e)
k	-	$k_1 = 0.04$ $k_2 = 0.05$	$k_1 = 0.05$ $k_2 = 0.06$	$k_1 = 0.06$ $k_2 = 0.07$	$k_1 = 0.07$ $k_2 = 0.08$
Total fraction of corrected intensity	0 %	9 %	11 %	13 %	15 %
R_{all}	0.1422	0.1237	0.1226	0.1259	0.1274
The strongest mF_o-DF_c peak on $\mathbf{t}_0$ catalytic Zn^{2+} ions (σ)	–11.3	–11.3	–12.0	–11.3	–12.0
Overall FOM	0.857	0.907	0.907	0.904	0.902
Average correlation coefficient (F_o, F_c)	0.9209	0.9311	0.9311	0.9280	0.9262

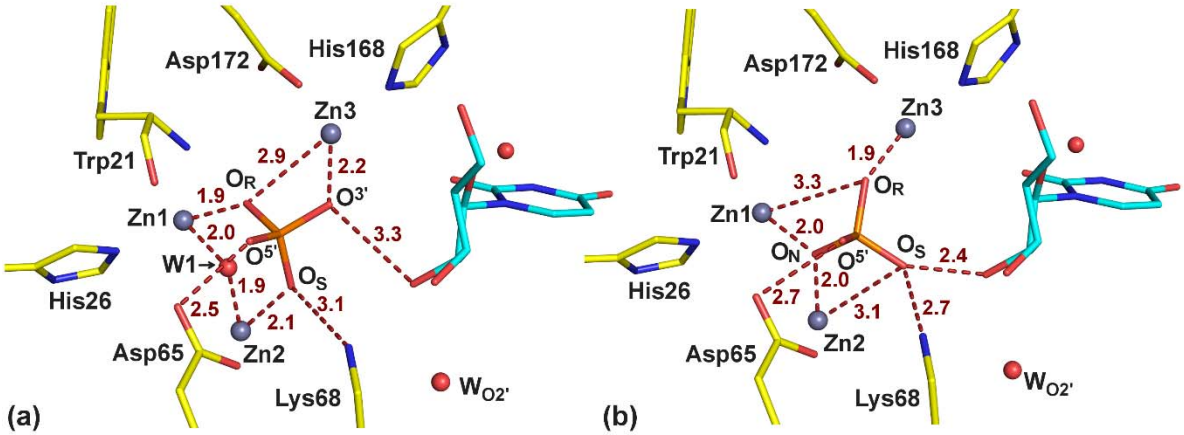

Figure S4 Two positions of phosphate in the active site of the S1-URI complex (alternative interpretations with occupancies 20 % and 30 %). The naming of the phosphate atoms corresponds to the naming in nucleotides. (a) Phosphate ion in the "leaving" position, which is probably also very similar to the pre-cleavage state (before inversion) with the nucleophile W1 centred between Zn1 and Zn2, oxygen O_R of phosphate coordinated between Zn1 and Zn3, oxygen O_S in contact with Zn2, oxygen $O^{3'}$ in contact with Zn3 and near the position of nucleoside uridine, and oxygen $O^{5'}$ in contact with Asp65 (2.5 Å to $O^{\delta1}$). (b) Position of phosphate in the post-cleavage state (after inversion), with oxygen O_N centred between Zn1 and Zn2, oxygen O_R in contact with Zn3, oxygen $O_{5'}$ in contact with Asp65 (2.7 Å to $O^{\delta1}$), and oxygen O_S in contact with Zn2 and stabilized by Lys68 and oxygen O2′ of the ribose moiety of URI. Phosphate contacts with neighbouring atoms are shown by red dashed lines and all interatomic distances are in Å. The molecular graphics was created using *PyMOL* (Schrödinger).

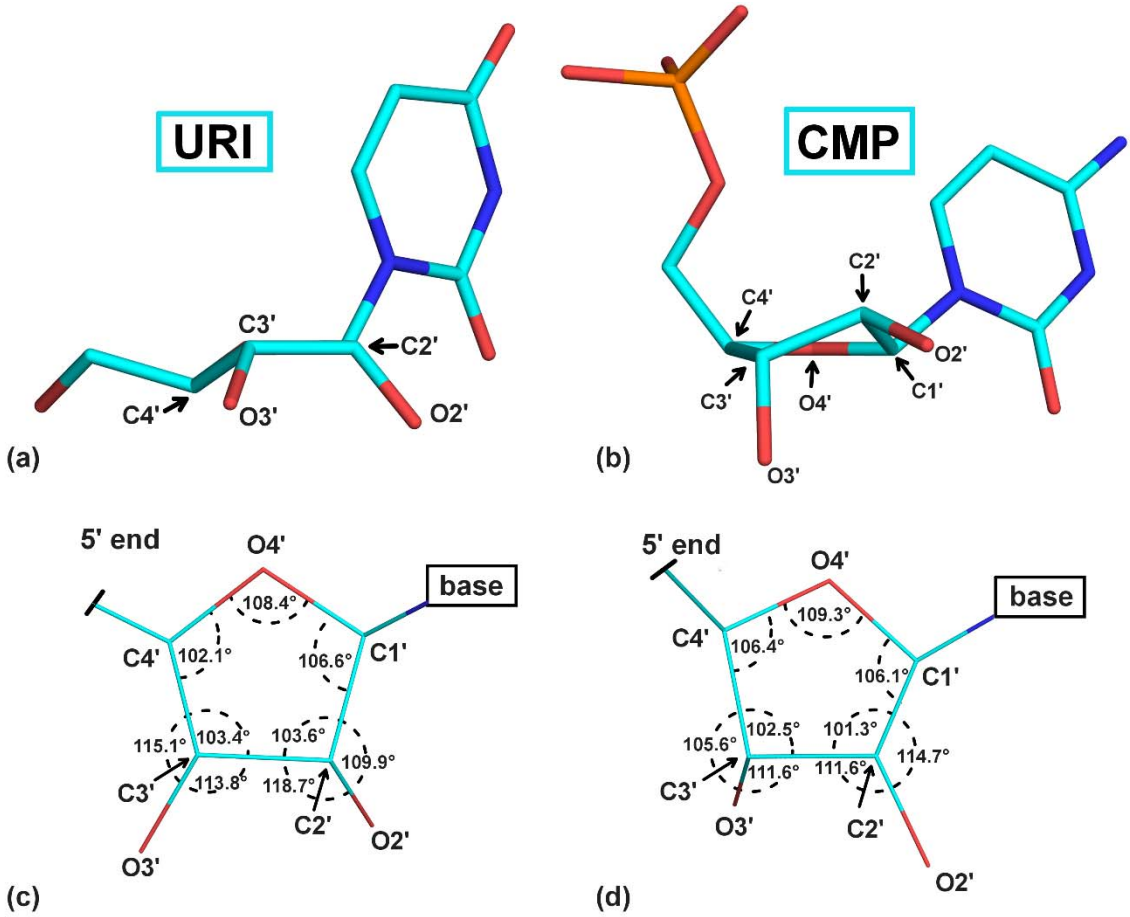

Figure S5 Conformation of the ribose moiety of ligands in the active site of S1 nuclease observed in the reported structures. (a) The C4′-exo conformation of ribose of URI, where the position of atom C4′ is out of the C3′-C2′-C1′-O4′ plane. The pseudorotational phase angle (Li and Szostak, 2014) is 57.34° as calculated using PROSIT (https://cactus.nci.nih.gov/prosit/) (b) The C2′-endo conformation of ribose of CMP, where the position of atom C2′ is on the same side with respect to the C1′-O4′-C4′ plane as the nucleobase and the 5′ end of nucleotide, while atom C3′ is on the other side. The pseudorotational phase angle (Li and Szostak, 2014) is 166.49° as calculated using PROSIT. (c) Valence angles of the ribose moiety of URI and (d) of CMP. The molecular graphics was created using *PyMOL* (Schrödinger).

References

Adams, P. D., Afonine, P. V., Bunkoczi, G., Chen, V. B., Davis, I. W., Echols, N., Headd, J. J., Hung, L.-W., Kapral, G. J., Grosse-Kunstleve, R. W., McCoy, A. J., Moriarty, N. W., Oeffner, R., Read, R. J., Richardson, D. C., Richardson, J. S., Terwilliger, T. C. & Zwart, P. H. (2010). *Acta Crystallographica Section D* **66**, 213-221.

Li, L. & Szostak, J. W. (2014). *J Am Chem Soc* **136**, 2858-2865.

Murshudov, G. N., Skubak, P., Lebedev, A. A., Pannu, N. S., Steiner, R. A., Nicholls, R. A., Winn, M. D., Long, F. & Vagin, A. A. (2011). *Acta Crystallogr D Biol Crystallogr* **67**, 355-367.